Accepted Manuscript

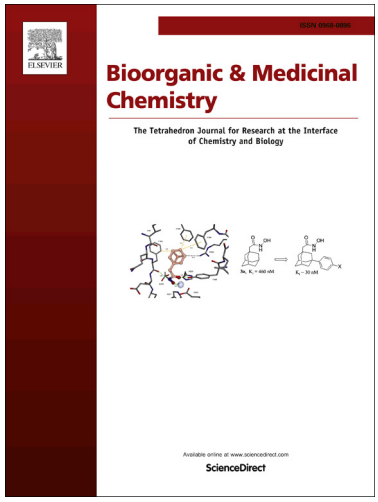

Synthesis and anti-hepatitis B virus activity of C4 amide-substituted isosteviol derivatives

Tsurng-Juhn Huang, Cheng-Lin Yang, Yu-Cheng Kuo, Yi-Chih Chang, Li-Ming Yang, Bo-Hon Chou, Shwu-Jiuan Lin

PII: S0968-0896(14)00922-5
DOI: http://dx.doi.org/10.1016/j.bmc.2014.12.064
Reference: BMC 11996

To appear in: *Bioorganic & Medicinal Chemistry*

Received Date: 2 November 2014
Revised Date: 25 December 2014
Accepted Date: 27 December 2014

Please cite this article as: Huang, T-J., Yang, C-L., Kuo, Y-C., Chang, Y-C., Yang, L-M., Chou, B-H., Lin, S-J., Synthesis and anti-hepatitis B virus activity of C4 amide-substituted isosteviol derivatives, *Bioorganic & Medicinal Chemistry* (2015), doi: http://dx.doi.org/10.1016/j.bmc.2014.12.064

Synthesis and anti-hepatitis B virus activity of C4 amide-substituted isosteviol derivatives

Tsurng-Juhn Huang[a], Cheng-Lin Yang[b], Yu-Cheng Kuo[c,d], Yi-Chih Chang[e], Li-Ming Yang[f,g], Bo-Hon Chou[g], Shwu-Jiuan Lin[g,h,*]

[a] *School of Medicine, China Medical University, Taichung 404, Taiwan*

[b] *Graduate Institute of Biomedical Sciences, National Chung Hsing University, Taichung 402, Taiwan*

[c] *Department of Radiation Oncology, China Medical University Hospital, Taichung 404, Taiwan*

[d] *Department of Biomedical Imaging and Radiological Science, China Medical University, Taichung 404, Taiwan*

[e] *Department of Medical Laboratory Science and Biotechnology, China Medical University, Taichung 404, Taiwan*

[f] *Division of Chinese Medicinal Chemistry, National Research Institute of Chinese Medicine, Ministry of Health and Welfare, Taipei 112, Taiwan*

[g] *Department of Pharmaceutical Sciences, School of Pharmacy, Taipei Medical University, Taipei 110, Taiwan*

[h] *PhD Program for the Clinical Drug Discovery from Botanical Herbs, College of Pharmacy, Taipei Medical University, Taipei 110, Taiwan*

Corresponding author. Tel.: +886 2 27361661x 6133; fax: +886 2 27390671.

E-mail address: shwu-lin@tmu.edu.tw (S.-J. Lin)

ABSTRACT

A series of novel isosteviol derivatives having C4-amide substituents were synthesized in order to test for antiviral effects against the hepatitis B virus (HBV) *in vitro*. Among them, IN-4 [*N*-(propylcarbonyl)-4α-amino-19-nor-*ent*-16-ketobeyeran] (**5**) exhibited inhibitory activity against secretion of HBsAg and HBeAg as well as inhibition of HBV DNA replication. Therefore, the mechanism of its antiviral activity was further analyzed using HBV-transfected Huh7 cells. Exposure to IN-4 produced minimal inhibitory effects on viral precore/pregenomic RNA expression. However, expression levels of the 2.4/2.1-kb preS/major S RNA of the viral surface gene significantly decreased, along with intracellular levels of HBV DNA. A promoter activity analysis demonstrated that IN-4 significantly inhibited viral X, S, and preS expression levels but not viral core promoter activities. In particular, IN-4 was observed to significantly inhibit HBV gene regulation by disrupting nuclear factor (NF)-κB-associated promoter activity. In addition, the nuclear expression of p65/p50 NF-κB member proteins was attenuated following IN-4 treatment, while cytoplasmic IκBα protein levels were enhanced. Meanwhile, IN-4 was observed to inhibit the binding activity of NF-κB to putative DNA elements. Furthermore, transfection of a p65 expression plasmid into Huh7 cells significantly reversed the inhibitory effect of IN-4 on HBV DNA levels, providing further evidence of the central role of NF-κB in its antiviral mechanism. It is therefore suggested that IN-4 inhibits HBV by interfering with the NF-κB signaling pathway, resulting in downregulation of viral gene expression and DNA replication.

Keywords: Isosteviol derivative, Antiviral effect, Hepatitis B virus, NF-κB

1. Introduction

The hepatitis B virus (HBV), the causative agent for hepatitis B, often leads to acute and chronic infections in humans.[1] Liver damage, including cirrhosis and hepatocellular carcinoma (HCC), occurs in approximately 80% of chronic HBV carriers.[2] Despite the development of a recombinant vaccine, which provides immunity against HBV, and the use of a specific hepatitis B immunoglobulin in susceptible populations, there are still more than 400 million chronic HBV carriers worldwide.[3] Although interferons and nucleotide analogs have previously been widely used to treat chronically infected patients, the rapid development of resistance and other undesirable side effects have prompted the search for alternate treatments. Recent studies focused on alterations in HBV gene regulation as a possible new treatment strategy.[4,5] This is a crucial issue for antiviral strategies because the focus is not on viral genome replication but on curing hepatitis B. Thus, continued development of new agents with different antiviral targets and mechanisms are urgently required to eradicate HBV in chronic carriers.

Isosteviol (*ent*-16-ketobeyeran-19-oic acid) (**1**) is obtained from the acid hydrolysis of the natural sweetener, stevioside, a constituent of *Stevia rebaudiana* (Bertoni) Bertoni (Compositae).[6,7] In view of its structural features and the fact that it possesses several biological properties,[5] various substituents have been introduced into the parent isosteviol molecule leading to novel compounds with new activities.[8,9] Isosteviol (**1**) possesses antiviral property against early antigen activation of the Epstein-Barr virus.[10] In our previous studies which searched for anti-HBV compounds, the ureide moiety substituted at the C4 of isosteviol (**1**) showed distinct action mechanisms from those

of typical HBV inhibitors.[5] In the literature, it is well known that amides are common structural features of many biologically active compounds.[11,12] That prompted us to continue exploring anti-HBV compounds with different targets and mechanisms. Several compounds bearing an amide moiety incorporated into C4 of isosteviol (**1**) were synthesized by reactions of amine **3** with various acid chlorides or benzoyl chlorides, and their anti-HBV activities were evaluated in HepG2 2.2.15 cells. Among them, IN-4 [*N*-(propylcarbonyl)-4α-amino-19-nor-*ent*-16-ketobeyeran] (**5**) (Scheme 1) was effective against secretion of the HBV surface antigen (HBsAg). Its IC_{50} of the inhibition to HBsAg secretion was 10.36 μg/ml, which was more potent than the reference drug lamivudine (49.13 μg/ml). Meanwhile, IN-4's IC_{50} (5.76 μg/ml) and SI (11.41) values of the inhibition of the replication of HBV DNA were higher than those of lamivudine (with an IC_{50} of 41 μg/ml and SI of 5) (Table 1). Thus, the inhibitory mechanism of IN-4 (**5**) against HBV in HBV-transfected Huh7 cells was investigated. In this report, we describe the synthesis of isosteviol derivatives by modifying C4 with various amide substituents, their activities against HBV, and the action mechanism of IN-4 (**5**).

2. Results

2.1. Synthesis and screening for anti-HBV activity

General synthesis of target compounds was accomplished as outlined in Scheme 1. The starting material of isosteviol (**1**) was prepared via a known strategy.[6] The diphenylphosphoryl azide (DPPA) was selected to convert the 19-COOH into an isocyanate **2**. Hydrolysis in concd HBr then afforded amine **3**. Thereafter, amine **3** was treated with various acid chlorides or benzoyl chlorides

in the presence of a catalytic amount of 4-dimethylaminopyridine (DMAP) to afford the target compounds **4**–**14** (Scheme 1). Structures of all compounds were characterized based on NMR and HRESIMS analyses. Subsequently, the synthesized compounds were examined for their anti-HBV activities, namely the abilities to inhibit the secretion of HBsAg and HBV e antigen (HBeAg) in HepG2 2.2.15 cells using lamivudine as a positive control. As shown in Table 1, the unsubstituted phenyl derivative **6** had only a weak activity (IC_{50}: 35.64 μg/ml) on inhibition of HBsAg secretion. Introduction of the electron-withdrawing halogen at 4-position of phenyl ring showed inhibition of HBsAg secretion, except for iodine. The fluoride substituted analogue **7** exhibited more potent anti-HBV activity than other halide substituted analogues (**8** and **9**). An electron-donating methyl group at 4-position of phenyl ring did not show anti-HBV activity. However, replacing methyl with ethyl group (**12**) at 4-position of phenyl ring led to exhibit good inhibitory activity against HBsAg (IC_{50}: 5.57 μg/ml; SI: 3.80) and HBeAg (IC_{50}: 7.38 μg/ml; SI: 2.87) secretion. Besides, when the ethyl group was replaced with the methoxy group (**13**), anti-HBV activity was decreased. Considering the effect of steric bulk, replacement of the phenyl moiety with propyl group afforded IN-4 (**5**), which exhibited significant inhibitory effect against secretion of HBsAg (IC_{50}: 10.36 μg/ml; SI: 6.34) and HBeAg (IC_{50}: 11.16 μg/ml; SI: 5.89). Although this series of compounds did not show any obvious SAR for anti-HBsAg and anti-HBeAg activity, three synthesized compounds **5**, **7**, and **12** showed significant inhibitory effects against HBsAg and HBeAg secretion. Thus, they were further selected to investigate inhibition of HBV DNA replication. The IC_{50} values for compounds **5**, **7**, and **12** against HBV DNA replication were 5.76, 7.44 and 11.2 μg/ml, respectively,

which were more potent than the commercial antiviral drug lamivudine (IC_{50}: 41 μg/ml). The selectivity index values of compounds **5**, **7**, and **12** were 11.41, 2.65, and 1.89, respectively. Of these compounds, IN-4 (**5**) was more potent than the positive control lamivudine (SI: 5). Based on the bioassay results, IN-4 (**5**) had the most potent anti-HBV activity within all of the tested compounds. Thus, further investigation of its mechanism of action against HBV was performed in HBV-transfected Huh7 cells.

2.2. Effect of IN-4 (5) on cell viability

To exclude the possibility that HBV production was suppressed by IN-4 (**5**) due to cellular cytotoxicity, the viability of HepG2 2.2.15 and Huh7 cells following IN-4 (**5**) exposure was tested using an MTS assay. Results indicated that IN-4 (**5**) caused significant cytotoxic effects at doses of > 20 μg/ml in HepG2 2.2.15 cells, but that no effect on HBV-transfected Huh7 cells at up to 160 μg/ml was observed (Fig. 1). Thus, a non-cytotoxic dose (< 10 μg/ml) was used for the antiviral treatment of HepG2 2.2.15 and HBV-transfected Huh7 cells.

2.3. Effects of IN-4 (5) on HBV virions and antigen secretion in HepG2 2.2.15 cells

The effect of IN-4 (**5**) on the expression of viral antigens was examined by measuring cellular secretion rates of HBsAg and HBeAg from HepG2 2.2.15 cells using an enzyme immunoassay (EIA). Following IN-4 (**5**) exposure at various concentrations (1, 5, and 10 μg/ml), both HBsAg and HBeAg secretions were significantly and similarly suppressed in dose-dependent manners compared to controls (Fig. 2A). The impact of IN-4 (**5**) on virion secretion was further examined by isolating viral DNA from conditioned medium of treated HepG2 2.2.15 cells and subjecting it to an

RT-PCR in order to detect extracellular viral DNA levels. Results showed that IN-4 (**5**) treatment significantly reduced secreted viral DNA levels in a dose-dependent manner compared to the controls (Fig. 2B).

2.4. Effect of IN-4 (5) on HBV gene expression

The effect of IN-4 (**5**) on HBV gene expression was determined by transiently transfecting Huh7 cells with the pHBV1.2 HBV genome-containing plasmid[13] and treating cells with three doses (1, 5, and 10 μg/ml) of IN-4 (**5**) for 2 days. A Northern blot analysis was performed to analyze HBV viral RNA expression levels as shown in Fig. 3A. IN-4 (**5**) treatment slightly reduced precore/pregenomic RNA levels but significantly reduced major S/preS RNA levels; the inhibition potential of IN-4 (**5**) was higher against surface RNA than against precore/pregenomic RNA. In addition, an immunoblot analysis was used to detect intracellular levels of HBV large and major surface (LHBsAg/SHBsAg) and core protein (HBcAg), and results indicated that IN-4 (**5**) significantly reduced LHBsAg, SHBsAg, and HBcAg protein levels compared to the vehicle controls (Fig. 3B). Furthermore, a Southern blot analysis confirmed that IN-4 (**5**) treatment significantly inhibited replication levels of HBV DNA in HBV-transfected Huh7 cells in a dose-dependent manner compared to the 3TC (lamivudine)-treated controls (Fig. 3C).

2.5. Effect of IN-4 (5) on HBV promoter activities

The regulatory effect of IN-4 (**5**) on HBV gene expression was examined by isolating and cloning four viral gene promoters into a pGL4.17 luciferase reporter vector[5] and testing the effect of IN-4 (**5**) on the promoter's activity level using a luciferase assay. In this study, pCore-Luc, pS-Luc

(S promoter), pPreS-Luc (preS promoter), or pX-Luc constructs were cotransfected with the pHBV1.2 HBV expression plasmid into Huh7 cells prior to the assay. Results showed that IN-4 (**5**) treatment significantly reduced S and preS promoter activities, whereas the inhibitory effects on Core and X promoter were not apparent (Fig. 4A). Four luciferase reporters that contained the NF-κB-, activator protein (AP)-1-, AP-2-, or interferon-sensitive response element (ISRE)-binding elements were transfected into Huh7 cells to determine whether IN-4 (**5**) inhibits HBV gene expression in a host's mediated cellular signaling pathways. Figure 4B shows that IN-4 (**5**) significantly inhibited NF-κB-containing promoter activity but did not affect AP-2- or ISRE-containing promoter activities. However, IN-4 (**5**) slightly upregulated AP-1-containing promoter activity (Fig. 4B).

2.6. Effects of IN-4 (5) on NF-κB and IκBα protein expression levels in Huh7 cells

Our results suggest that NF-κB plays a regulatory role in HBV gene expression. In order to further confirm this, Huh7 cells were transfected with pHBV1.2, treated with IN-4 (**5**), and analyzed by Western blotting. Results showed that IN-4 (**5**) treatment reduced nuclear p65/p50 NF-κB protein expression and reduced phosphorylated NF-κB p65 levels in nuclei (Fig. 5A). However, the cytoplasmic IκBα level was significantly enhanced. An EMSA provided support for this finding by demonstrating that IN-4 (**5**) treatment significantly reduced the binding activity of NF-κB to the consensus DNA-binding sequence in a dose-dependent manner (Fig. 5B).

2.7. NF-κB is essential for the inhibitory effects of IN-4 (5) on HBV

To further examine whether the regulatory effect of IN-4 (**5**) on HBV is mediated through

inhibition of the NF-κB signaling pathway, a p65 expression plasmid was cotransfected with pHBV1.2 into Huh7 cells and treated with IN-4 (**5**) (10 μg/ml). HBV DNA from the culture medium was extracted, and an RT-PCR analysis showed that an increase in the p65 expression dose (0.5 and 2.5 μg) was able to reverse the inhibitory effect of IN-4 (**5**) on the HBV DNA level compared to transfection with the empty vector (Fig. 6).

3. Discussion

The development of mechanistically novel anti-HBV drugs that are able to alleviate the problems associated with current therapies poses a major challenge.[14] This study observed that a synthesized isosteviol derivative, IN-4 (**5**), inhibited viral activity by decreasing certain HBV DNA, RNA, and protein expression levels in Huh7 cells. In particular, IN-4 (**5**) was able to eliminate the expression of both the large and major viral surface antigen and viral core proteins. S/preS HBV viral transcripts were also observed to have been significantly decreased by IN-4 (**5**) treatment. In addition, a Southern blot analysis revealed that IN-4 (**5**) significantly inhibited the production of the replicated DNA intermediate of HBV. An examination of HBV promoter activity demonstrated that the X, S, and preS promoters were attenuated by IN-4 (**5**), but core promoter activity was not affected. These results suggest that IN-4 (**5**) acts by inhibiting HBV gene promoter activity. To examine the mechanisms involved in the ability of IN-4 (**5**) to affect a host's cellular signaling pathways, transcriptional activities of four major signaling pathways, AP-1, AP-2, NF-κB, and ISRE, were analyzed using a promoter-reporter assay. After transfection and treatment, IN-4 (**5**) decreased NF-κB promoter activity and slightly induced AP-1 promoter activity, but there were no

effects on the AP-2 or ISRE promoters. This suggests that IN-4 (**5**) specifically regulates the NF-κB signaling pathway in HBV-infected host cells. Expression levels of nuclear NF-κB p65/p50 proteins and the phosphorylated p65 protein were observed to decrease following IN-4 (**5**) exposure, whereas the IκBα protein level increased with the same treatment in a dose-dependent manner. These results suggest that IN-4 (**5**) could potentially enhance IκBα, and cause p65/p50 NF-κB exportation from nuclei to the cytoplasm, thus attenuating nuclear p65 phosphorylation in subsequent activation. To further examine the potential influence of IN-4 (**5**) on the binding activity of NF-κB to DNA-binding elements, the consensus NF-κB-binding sequence was synthesized and used for an EMSA analysis. As observed in Figure 5B, IN-4 (**5**) treatment significantly decreased the binding activity of NF-κB to the DNA element in a dose-dependent manner.

To further investigate the interplay among IN-4 (**5**), NF-κB regulation, HBV gene expression, and viral propagation, a pCMV-p65 NF-κB expression plasmid was cotransfected with pHBV1.2 into Huh7 cells. The secreted HBV viral particles were subjected to a Southern blot analysis, which showed significant inhibition of viral particle secretion following IN-4 (**5**) treatment. However, this effect was reversed when cells were cotransfected with an increasing dose (0.5 and 2.5 μg) of the pCMV-p65 plasmid using the same treatment. There was no difference in secreted levels of HBV DNA at the maximum transfection dose of the pCMV-p65 plasmid combined with IN-4 (**5**) treatment compared to untreated controls. This result provides further evidence that IN-4 (**5**) mediates its effect on HBV gene expression and DNA replication via the NF-κB signaling pathway.

4. Conclusions

This study demonstrated that IN-4 (**5**) inhibits HBV gene expression and viral DNA replication by interfering with the NF-κB signaling pathway in host cells. Previous studies proposed that activation of the NF-κB pathway can be mediated by viral proteins,[15] and that inhibiting NF-κB activation in HBV-infected cells may provide possible treatment.[16–19] This study was unable to determine whether IN-4 (**5**) was directly involved in regulating viral promoter activities or if it just disrupted feedback activation of viral proteins involved in NF-κB gene expression and activation.[17,18,20] Thus, further work on this aspect of the antiviral activities of IN-4 (**5**) is warranted. In conclusion, a novel compound for the potential treatment of HBV infection was described, and its basic mechanism of action was elucidated. The results will aid in the development of novel anti-HBV compounds based on isosteviol and provide insight into anti-HBV mechanism.

5. Experimental

5.1. Chemistry

5.1.1. General

Melting points were determined using a Yanagimoto micromelting point apparatus and are uncorrected. Optical rotations were determined on a JASCO DIP-1020 digital polarimeter. ^{1}H, ^{13}C NMR, and DEPT spectra were recorded on a Bruker Avance DRX 500 spectrometer. Chemical shifts are reported in parts per million (ppm) with respect to the corresponding solvent as the internal standard, and coupling constants (*J*) are in Hertz (Hz). ESI-MS spectra were recorded using a VG platform electrospray mass spectrometer and a Bruker maXis impact QTOF mass spectrometer. Spots for all compounds were detected by spraying with Dragendorff's reagent and

10% H_2SO_4 followed by heating.

5.1.2. Synthesis of compounds 4–14 and anti-HBV assay

Isosteviol (**1**) was obtained by acid hydrolysis of stevioside.[6] The key intermediate of amine **3** was prepared by reacting **1** with DPPA in the presence of benzene to afford isocyanate **2** (yield: 86%). Hydrolysis of **2** in concd HBr then afforded amine **3** (yield: 70%). Subsequently, a solution of **3** (0.3 mmole), DMAP (0.78 mmole), acyl chlorides or benzoyl chlorides (1 mmole), and triethylamine (400 μl) in dimethylformamide (5 ml) was stirred overnight at room temperature. The reaction mixture was respectively washed with 1 N HCl, H_2O, and saturated $NaHCO_3$. The resulting solution was extracted with EtOAc. The combined organic layers were dried and filtered. Removal of the solvent under reduced pressure afforded a crude residue. It was crystallized using H_2O-MeOH to afford compounds **4**–**14**. Structures of all compounds were characterized by NMR and HRESIMS analyses. Inhibitory activity against HBV was performed as described previously.[21]

5.1.2.1. 4α-Amino-19-nor-*ent*-16-ketobeyeran (3)

White crystals, yield: 70%; mp 210-212 °C [lit. 273 °C (HCl)][22]; $[\alpha]^{25}_{D}$ −45.5 (*c* 1.65, CH_3OH); ^{1}H NMR (500 MHz, CD_3OD): δ 2.61 (dd, *J* = 15.5, 3.0 Hz, 1H), 1.90 (d, *J* = 15.5 Hz, 1H), 1.84 (m, 1H), 1.70-1.78 (m, 5H), 1.55-1.67 (m, 5H), 1.45-1.51 (m, 3H), 1.37-1.39 (m, 2H), 1.36 (s, 3H), 1.23 (m, 1H), 1.06 (m, 1H), 0.98 (s, 3H), 0.95 (s, 3H); ^{13}C NMR (125 MHz, CD_3OD): δ 224.5, 57.1, 55.5, 54.9, 54.6, 49.8, 49.4, 41.1, 40.4, 38.6, 38.4, 38.1, 38.0, 28.3, 20.9, 20.2, 20.1, 17.8, 14.4; HRESIMS *m/z* 290.2482 $[M + H]^+$ (calcd for $C_{19}H_{32}NO$, 290.2484).

5.1.2.2. *N*-(Ethylcarbonyl)-4α-amino-19-nor-*ent*-16-ketobeyeran (4)

White crystals, yield: 75.4%; mp 143–145 °C; $[\alpha]^{25}_{D}$ –63.3 (*c* 1.1, CH_3OH); ^{1}H NMR (500 MHz, C_5D_5N): δ 4.90 (s, 1H), 3.10 (br d, *J* = 13.5 Hz, 1H), 2.63 (dd, *J* = 18.4, 3.5 Hz, 1H), 2.24 (q, *J* = 15.2, 7.6 Hz, 2H), 1.75-1.78 (m, 2H), 1.50-1.56 (m, 5H), 1.56 (s, 3H), 1.41-1.45 (m, 3H), 1.31-1.33 (m, 3H), 1.15 (t, *J* = 7.7 Hz, 3H), 1.08-1.16 (m, 3H), 1.02 (s, 3H), 0.99 (s, 3H), 0.93 (m, 1H), 0.78 (m, 1H); ^{13}C NMR (125 MHz, C_5D_5N): δ 220.8, 172.8, 56.4, 55.7, 54.9, 54.2, 48.8, 48.6, 41.0, 39.4, 39.2, 37.7, 37.3, 36.4, 30.9, 27.4, 20.2, 20.1, 19.8, 18.1, 14.9, 10.5; HRESIMS *m*/*z* 346.2751 $[M + H]^+$ (calcd for $C_{22}H_{36}NO_2$, 346.2746).

5.1.2.3. *N*-(Propylcarbonyl)-4α-amino-19-nor-*ent*-16-ketobeyeran (5) (IN-4)

White crystals, yield: 72.5%; mp 158-160 °C; $[\alpha]^{24}_{D}$ –67.2 (*c* 1.2, CH_3OH); ^{1}H NMR (500 MHz, C_5D_5N): δ 5.82 (s, 1H), 3.14 (br d, *J* = 13.6 Hz, 1H), 2.63 (dd, *J* = 18.4, 3.6 Hz, 1H), 2.19 (t, *J* = 7.3 Hz, 2H), 1.67-1.79 (m, 5H), 1.50-1.57 (m, 4H), 1.57 (s, 3H), 1.43-1.45 (m, 3H), 1.31-1.34 (m, 3H), 1.07-1.11 (m, 3H), 1.02 (s, 3H), 1.01 (s, 3H), 0.94 (m, 1H), 0.90 (t, *J* = 7.4 Hz, 3H), 0.78 (td, *J* = 13.0, 4.0 Hz, 1H); ^{13}C NMR (125 MHz, C_5D_5N): δ 220.7, 172.0, 56.4, 55.8, 54.9, 54.2, 48.8, 48.6, 41.0, 39.8, 39.4, 39.2, 37.7, 37.3, 36.4, 27.4, 20.2, 20.1, 19.7, 19.7, 18.1, 14.9, 14.0; HRESIMS *m*/*z* 360.2903 $[M + H]^+$ (calcd for $C_{23}H_{38}NO_2$, 360.2903).

5.1.2.4. *N*-(Phenylcarbonyl)-4α-amino-19-nor-*ent*-16-ketobeyeran (6)

White crystals, yield: 70.1%; mp 150–152 °C; $[\alpha]^{25}_{D}$ –68.9 (*c* 1.3, CH_3OH); ^{1}H NMR (500 MHz, C_5D_5N): δ 8.04 (m, 2H), 7.44 (m, 3H), 6.31 (s, 1H), 3.26 (br d, *J* = 13.7 Hz, 1H), 2.62 (dd, *J* = 18.5, 3.5 Hz, 1H), 1.80 (m, 1H), 1.76 (d, *J* = 18.5 Hz, 1H), 1.65 (s, 3H), 1.43-1.59 (m, 8H), 1.28-1.34 (m, 3H), 1.09-1.18 (m, 3H), 1.05 (s, 3H), 1.02 (s, 3H), 1.00 (m, 1H), 0.81 (m, 1H); ^{13}C

NMR (125 MHz, C_5D_5N): δ 220.8, 166.3, 136.9, 131.4, 129.0, 129.0, 127.2, 127.2, 56.4, 56.4, 54.9, 54.2, 48.8, 48.6, 40.9, 39.3, 39.0, 37.7, 37.3, 36.1, 27.3, 20.2, 20.1, 19.7, 18.1, 15.2; HRESIMS *m*/*z* 394.2748 $[M + H]^+$ (calcd for $C_{26}H_{36}NO_2$, 394.2746)

5.1.2.5. *N*-(*p*-Fluorophenylcarbonyl)-4α-amino-19-nor-*ent*-16-ketobeyeran (7)

White crystals, yield: 28.1%; mp 193−195 °C; $[\alpha]^{25}_D$ −68.2 (*c* 1.25, CH_3OH); ^1H NMR (500 MHz, C_5D_5N): δ 8.04 (m, 2H), 7.20 (t, *J* = 8.6 Hz, 2H), 6.33 (s, 1H), 3.24 (br d, *J* = 13.7 Hz, 1H), 2.61 (dd, *J* = 18.4, 2.8 Hz, 1H), 1.80 (m, 1H), 1.75 (d, *J* = 18.4 Hz, 1H), 1.65 (s, 3H), 1.41-1.62 (m, 8H), 1.27-1.35 (m, 3H), 1.04-1.19 (m, 4H), 1.07 (s, 3H), 1.03 (s, 3H), 0.83 (td, *J* = 13.0, 4.0 Hz, 1H); ^{13}C NMR (125 MHz, C_5D_5N): δ 220.7, 165.7, 165.3, 163.7, 133.2, 129.8, 129.7, 115.8, 115.7, 56.5, 56.4, 54.9, 54.1, 48.8, 48.6, 40.9, 39.3, 39.0, 37.7, 37.3, 36.1, 27.2, 20.2, 20.1, 19.7, 18.1, 15.2; HRESIMS *m*/*z* 412.2654 $[M + H]^+$ (calcd for $C_{26}H_{35}NO_2F$, 412.2652).

5.1.2.6. *N*-(*p*-Chlorophenylcarbonyl)-4α-amino-19-nor-*ent*-16-ketobeyeran (8)

White crystals, yield: 52%; mp 246−248 °C; $[\alpha]^{24}_D$ −25.0 (*c* 1.15, C_5H_5N); ^1H NMR (500 MHz, C_5D_5N): δ 7.97 (d, *J* = 8.5 Hz, 2H), 7.46 (d, *J* = 8.5 Hz, 2H), 6.36 (s, 1H), 3.22 (br d, *J* = 13.8 Hz, 1H), 2.60 (dd, *J* = 18.4, 3.6 Hz, 1H), 1.80 (m, 1H), 1.74 (d, *J* = 18.4 Hz, 1H), 1.65 (s, 3H), 1.62 (m, 1H), 1.43-1.59 (m, 8H), 1.30-1.39 (m, 3H), 1.02-1.19 (m, 3H), 1.04 (s, 3H), 1.02 (s, 3H), 0.82 (m, 1H); ^{13}C NMR (125 MHz, C_5D_5N): δ 220.7, 165.3, 137.1, 135.8, 129.0, 129.0, 129.0, 129.0, 56.6, 56.4, 54.9, 54.1, 48.7, 48.6, 40.9, 39.3, 39.0, 37.7, 37.3, 36.1, 27.2, 20.2, 20.1, 19.7, 18.1, 15.1; HRESIMS *m*/*z* 428.2358 $[M + H]^+$ (calcd for $C_{26}H_{35}NO_2Cl$, 428.2356).

5.1.2.7. *N*-(*p*-Bromophenylcarbonyl)-4α-amino-19-nor-*ent*-16-ketobeyeran (9)

White crystals, yield: 50.1%; mp 197–199 °C; $[\alpha]^{25}_{D}$ –23.5 (*c* 1.0, C_5H_5N); ^{1}H NMR (500 MHz, C_5D_5N): δ 7.90 (d, *J* = 8.4 Hz, 2H), 7.62 (d, *J* = 8.4 Hz, 2H), 6.36 (s, 1H), 3.22 (br d, *J* = 13.6 Hz, 1H), 2.60 (dd, *J* = 18.4, 3.5 Hz, 1H), 1.80 (m, 1H), 1.74 (d, *J* = 18.4 Hz, 1H), 1.65 (s, 3H), 1.62 (m, 1H), 1.43-1.58 (m, 8H), 1.31-1.34 (m, 3H), 1.03-1.19 (m, 3H), 1.06 (s, 3H), 1.03 (s, 3H), 0.82 (m, 1H); ^{13}C NMR (125 MHz, C_5D_5N): δ 220.7, 165.5, 132.1, 132.1, 132.1, 129.2, 129.2, 125.8, 56.6, 56.4, 54.9, 54.2, 48.8, 48.6, 40.9, 39.3, 39.0, 37.7, 37.3, 36.1, 27.2, 20.2, 20.2, 19.7, 18.1, 15.2; HRESIMS *m*/*z* 472.1865 $[M + H]^+$ (calcd for $C_{26}H_{35}NO_2Br$, 472.1851).

5.1.2.8. *N*-(*p*-Iodophenylcarbonyl)-4α-amino-19-nor-*ent*-16-ketobeyeran (10)

White crystals, yield: 49.6%; mp 278–280 °C; $[\alpha]^{24}_{D}$ –25.1 (*c* 1.9, C_5H_5N); ^{1}H NMR (500 MHz, C_5D_5N): δ 7.85 (d, *J* = 8.5 Hz, 2H), 7.76 (d, *J* = 8.5 Hz, 2H), 6.36 (s, 1H), 3.22 (br d, *J* = 13.7 Hz, 1H), 2.61 (dd, *J* = 18.5, 3.6 Hz, 1H), 1.80 (m, 1H), 1.75 (d, *J* = 18.5 Hz, 1H), 1.65 (s, 3H), 1.43-1.59 (m, 7H), 1.32-1.35 (m, 3H), 1.11-1.19 (m, 4H), 1.07 (s, 3H), 1.03 (s, 3H), 1.00 (m, 1H), 0.82 (td, *J* = 11.0, 3.0 Hz, 1H); ^{13}C NMR (125 MHz, C_5D_5N): δ 220.7, 165.7, 138.1, 138.1, 136.3, 129.0, 129.0, 98.8, 56.6, 56.4, 54.9, 54.2, 48.7, 48.6, 40.9, 39.3, 39.0, 37.7, 37.3, 36.1, 27.2, 20.2, 20.1, 19.7, 18.1, 15.2; HRESIMS *m*/*z* 520.1707 $[M + H]^+$ (calcd for $C_{26}H_{35}NO_2I$, 520.1712).

5.1.2.9. *N*-(*p*-Methylphenylcarbonyl)-4α-amino-19-nor-*ent*-16-ketobeyeran (11)

White crystals, yield: 40%; mp 96–98 °C; $[\alpha]^{24}_{D}$ –71.6 (*c* 1.65, CH_3OH); ^{1}H NMR (500 MHz, C_5D_5N): δ 7.98 (d, *J* = 8.0 Hz, 2H), 7.24 (d, *J* = 8.0 Hz, 2H), 6.28 (s, 1H), 3.27 (br d, *J* = 13.5 Hz, 1H), 2.62 (dd, *J* = 18.5, 3.5 Hz, 1H), 1.78 (m, 1H), 1.76 (d, *J* = 18.5 Hz, 1H), 1.66 (s, 3H), 1.43-1.60 (m, 9H), 1.31-1.34 (m, 4H), 1.11-1.18 (m, 4H), 1.06 (s, 3H), 1.03 (s, 3H), 0.99 (m, 1H),

0.82 (td, *J* = 18.5, 3.5 Hz, 1H); ^{13}C NMR (125 MHz, C_5D_5N): δ 220.7, 166.2, 141.6, 134.1, 129.6, 129.6, 127.3, 127.3, 56.4, 56.3, 54.9, 54.2, 48.8, 48.6, 40.9, 39.3, 39.0, 37.7, 37.3, 36.0, 27.3, 21.2, 20.2, 20.1, 19.7, 18.1, 15.2; HRESIMS *m*/*z* 408.2903 $[M + H]^+$ (calcd for $C_{27}H_{38}NO_2$, 408.2903).

5.1.2.10. *N*-(*p*-Ethylphenylcarbonyl)-4α-amino-19-nor-*ent*-16-ketobeyeran (12)

White crystals, yield: 41.4%; mp 174–176 °C; $[\alpha]^{25}_D$ –68.7 (*c* 1.3, CH_3OH); ^{1}H NMR (500 MHz, C_5D_5N): δ 7.99 (d, *J* = 8.0 Hz, 2H), 7.27 (d, *J* = 8.0 Hz, 2H), 6.30 (s, 1H), 3.27 (br d, *J* = 13.7 Hz, 1H), 2.64 (dd, *J* = 18.5, 3.5 Hz, 1H), 2.55 (q, *J* = 7.6 Hz, 2H), 1.76-1.83 (m, 1H), 1.78 (d, *J* = 18.5, 1H), 1.67 (s, 3H), 1.44-1.61 (m, 8H), 1.31-1.36 (m, 3H), 1.16-1.19 (m, 4H), 1.11 (t, *J* = 7.6 Hz, 3H), 1.08 (s, 3H), 1.03 (s, 3H), 0.83 (m, 1H); ^{13}C NMR (125 MHz, C_5D_5N): δ 220.8, 166.3, 147.8, 134.4, 128.5, 128.5, 127.4, 127.4, 56.4, 56.3, 54.9, 54.1, 48.8, 48.6, 40.9, 39.3, 39.0, 37.7, 37.3, 36.0, 28.9, 27.3, 20.2, 20.1, 19.6, 18.1, 15.6, 15.2; HRESIMS *m*/*z* 422.3013 $[M + H]^+$ (calcd for $C_{28}H_{40}NO_2$, 422.3059).

5.1.2.11. *N*-(*p*-Methoxyphenylcarbonyl)-4α-amino-19-nor-*ent*-16-ketobeyeran (13)

White crystals, yield: 56%; mp 233–235 °C; $[\alpha]^{25}_D$ –23.5 (*c* 1.05, C_5H_5N); ^{1}H NMR (500 MHz, C_5D_5N): δ 8.04 (d, *J* = 8.5 Hz, 2H), 7.02 (d, *J* = 8.5 Hz, 2H), 6.24 (s, 1H), 3.67 (s, 3H), 3.27 (br d, *J* = 13.5 Hz, 1H), 2.62 (dd, *J* = 18.0, 3.5 Hz, 1H), 1.79 (m, 1H), 1.75 (d, *J* = 18.0 Hz, 1H), 1.66 (s, 3H), 1.41-1.60 (m, 9H), 1.26-1.36 (m, 3H), 1.09-1.20 (m, 2H), 1.07 (s, 3H), 1.02 (s, 3H), 0.99 (m, 1H), 0.80 (td, *J* = 13.0, 3.5 Hz, 1H); ^{13}C NMR (125 MHz, C_5D_5N): δ 220.7, 165.8, 162.3, 129.1, 129.1, 129.0, 114.2, 114.2, 56.4, 56.2, 55.3, 54.9, 54.1, 48.7, 48.5, 40.9, 39.3, 39.0, 37.6, 37.2, 36.0, 27.3, 20.2, 20.1, 19.6, 18.1, 15.2; HRESIMS *m*/*z* 424.2853 $[M + H]^+$ (calcd for

$C_{27}H_{38}NO_3$, 424.2852).

5.1.2.12. *N*-(*p*-Cyanophenylcarbonyl)-4α-amino-19-nor-*ent*-16-ketobeyeran (14)

White crystals, yield: 60.3%; mp 215–217 °C; $[\alpha]^{25}_D$ –69.6 (*c* 1.2, CH_3OH); ^{1}H NMR (500 MHz, C_5D_5N): δ 8.04 (d, *J* = 8.3 Hz, 2H), 7.76 (d, *J* = 8.3 Hz, 2H), 6.55 (s, 1H), 3.19 (br d, *J* = 13.6 Hz, 1H), 2.60 (dd, *J* = 18.0, 3.5 Hz, 1H), 1.83 (m, 1H), 1.70 (d, *J* = 18.0 Hz, 1H), 1.68 (m, 1H), 1.66 (s, 3H), 1.43-1.59 (m, 7H), 1.30-1.40 (m, 3H), 1.02-1.22 (m, 4H), 1.08 (s, 3H), 1.03 (s, 3H), 0.84 (m, 1H); ^{13}C NMR (125 MHz, C_5D_5N): δ 220.7, 165.1, 140.7, 132.8, 132.8, 128.1, 128.1, 118.8, 114.7, 56.9, 56.4, 54.9, 54.2, 48.7, 48.6, 40.9, 39.3, 39.0, 37.7, 37.3, 36.2, 27.2, 20.2, 20.2, 19.8, 18.1, 15.2; HRESIMS *m*/*z* 419.2700 $[M + H]^+$ (calcd for $C_{27}H_{35}N_2O_2$, 419.2699).

5.2. Biological evaluation

5.2.1. Materials

Anti-preS2 surface, anti-HBcAg, anti-NF-κB (p65/p50), and anti-IκBα antibodies were purchased from Santa Cruz Biotechnology (Santa Cruz, CA, USA). The antibody against proliferating cell nuclear antigen (PCNA) was purchased from Cell Signaling Technology (Danvers, MA, USA). The DIG high prime DNA labeling and detection starter kit was obtained from Roche (Mannheim, Germany), while the Power SYBR Green PCR master mix was purchased from Applied Biosystems (Foster City, CA, USA). The QIAquick gel extraction kit was purchased from Qiagen (Valencia, CA, USA), and the dual-luciferase reporter assay kit was purchased from Promega (Madison, WI, USA). The Trizol® total RNA isolation solution and the Lipofectamine 2000 transfection reagent were obtained from Invitrogen (Carlsbad, CA, USA). Lamivudine

(2′,3′-dideoxy-3′-thiacytidine, commonly known as 3TC) and the anti-α-tubulin antibody were purchased from Sigma (St. Louis, MO, USA). pNF-κB-Luc, pAP-1-Luc, pAP-2-Luc, and p-ISRE-Luc promoter-luciferase reporter constructs from Stratagene (La Jolla, CA, USA) were provided by Dr. Cheng-Wen Lin (Department of Medical Laboratory Science and Biotechnology, China Medical University, Taichung, Taiwan). The pCMV-p65 expression plasmid was provided by Dr. Chen-Kung Chou (Department of Biomedical Sciences, Chang Gung University, Taoyuan, Taiwan).

5.2.2. Cell culture

HepG2 2.2.15 cells, derived from HepG2 human hepatocellular carcinoma cells, were stably transfected with a head-to-tail HBV DNA dimer[23] and were maintained in MEM with heat-inactivated 10% fetal bovine serum (FBS) and 1% antibiotics. In parallel experiments, human Huh7 hepatoma cells were maintained in Dulbecco's modified Eagle medium (DMEM) supplemented with heat-inactivated 10% FBS and 1% antibiotics. HepG2 2.2.15 and Huh7 cells were both grown at 37 °C in a humidified atmosphere of 5% CO_2 and 95% air.

5.2.3. Cell viability assay

The cytotoxic effects of IN-4 (**5**) were determined using a CellTiter 96® AQ_{ueous} one solution cell proliferation assay kit (MTS) (Promega, Madison, WI, USA). In order to pinpoint the toxicity limits in HepG2 2.2.15 and Huh7 cells, they were plated into 96-well plates at a density of 4×10^4 cells/ml for 24 h. Cells were then treated with serial dilutions of IN-4 (**5**), ranging 2.5–160 μg/ml, and the mixture was incubated for 3 days. Cell toxicity was measured according to the

manufacturer's protocol. All measurements were performed in four replicates, and results are presented as relative percentages over that of the control group.

5.2.4. Determination of HBsAg and HBeAg expression levels

After treating HepG2 2.2.15 cells or HBV-transfected Huh7 cells, levels of the HBsAg and HBeAg proteins were measured in culture media using an EIA kit (Johnson and Johnson, Skillman, NJ, USA) according to the manufacturer's instructions.

5.2.5. Plasmid construction

All plasmid constructs were produced using standard recombinant DNA techniques.[24] The pHBV1.2 plasmid containing a 1.2-fold HBV adw2 serotype genome (nt 2186~1986) was cloned into the *Eco*RI site of pGEM-7Zf (+) (Promega, Madison, WI, USA)[13] which was kindly provided by Dr. Cheng-Chan Lu (Department of Pathology, National Cheng-Kung University, Tainan, Taiwan). The four viral promoter-reporter plasmids were constructed by amplifying the HBV genomic fragments that corresponded to the Core (nt1636−1851), S (nt3114−220), PreS (nt2438−2855), and X (nt1071−1357) gene promoter regions with a polymerase chain reaction (PCR) that used the pHBV1.2 plasmid as a template. These amplicons were inserted into *Sac*I/*Xho*I sites of the pGL4.17 luciferase-reporter expression vector (Promega) as previously described.[5] All of the DNA sequences were verified using restriction enzyme digestion and direct sequencing.

5.2.6. Promoter-reporter activity assay

Cells were plated into 24-well culture plates, transfected with promoter-reporter constructs (1 μg/well) and pRL-SV40 in serum-free DMEM for 24 h, washed with 1× phosphate-buffered saline

(PBS), incubated in DMEM supplemented with 2% FBS, and treated with or without IN-4 (**5**) (10 μg/ml) for 2 days. Luciferase assays were performed according to the manufacturer's instructions (Promega). The promoter-reporter construct transfection consisted of cotransfecting the pRL-SV40 Renilla luciferase expression plasmid (0.02 μg/well) (Promega) and using it to normalize the basal level of luciferase activity.

5.2.7. Transfection

Huh7 cells were seeded in 60-mm dishes at 4×10^4 cells/ml for 24 h. Cells were then transfected with the pHBV1.2 plasmid using Lipofectamine 2000 (Invitrogen, Carlsbad, CA, USA) in DMEM containing 10% FBS for 2 days, as per the manufacturer's protocol. Cells were then treated with IN-4 (**5**) for a further 2 days.

5.2.8. Analysis of intracellular HBV RNA by Northern blotting

Total RNA from the treated cells was extracted using Trizol® isolation buffer (Invitrogen) according to the manufacturer's protocol. Five micrograms of total RNA was denatured, separated on a 1.0% agarose gel using a commercial kit (Amresco, Solon, OH, USA), and transferred to a positively charged Hybond N^+ nylon membrane (GE Healthcare, Amersham, Buckinghamshire, UK). After UV cross-linking, the membrane was hybridized with a DIG-labeled full-length HBV genome probe, washed, and exposed to X-ray film. In brief, the full-length HBV probe was produced by the restriction enzymatic digestion of the pHBV2 plasmid with *Eco*RI,[25] followed by purification and labeling with a DIG high prime DNA labeling kit (Roche). Total RNA was normalized by hybridizing the membrane with a glyceraldehyde-3-phosphate dehydrogenase

(GAPDH) probe which was produced by *Pst* I digestion of the pGAPDH plasmid (provided by Dr. Hsiao-Sheng Liu from the Graduate Institute of Microbiology and Immunology, National Cheng-Kung University). Variations in the transfection efficiency were controlled by cotransfecting Huh7 cells with pCMV-β (Clontech, Palo Alto, CA, USA), which contained the CMV immediate-early promoter driving the β-galactosidase (β-*gal*) gene.

5.2.9. Southern blot and real-time PCR analysis of intracellular HBV-DNA synthesis

Cellular encapsidated HBV DNA was extracted from core particles, fractionated on 1.0% agarose gels, and transferred onto Hybond N^+ membranes (GE Healthcare) as described by Pugh et al.[26] HBV DNA was detected by a Southern blot analysis using a DIG-labeled full-length HBV probe. In addition, virion HBV DNA from conditioned media that had been either untreated or treated with IN-4 (**5**) or lamivudine (3TC) was isolated and subjected to a Southern blot analysis as described above. A real-time PCR analysis of HBV DNA used 5′-AGGAGGCTGTAGGCATAAATTGG-3′ as the forward primer and 5′-CAGCTTGGAGGCTTGAACAGT-3′ as the reverse primer.[27] The PCR were performed using SYBR Green PCR master mix, and the reaction protocol was as follows: initial denaturation at 50 °C for 2 min and 95 °C for 10 min, followed by 45 cycles of amplification at 95 °C for 15 s and annealing/extending at 58 °C for 1 min.

5.2.10. Sodium dodecylsulfate (SDS)-polyacrylamide gel electrophoresis (PAGE) and Western blot analyses of intracellular viral antigens and cellular signaling proteins

Whole-cell protein extracts of Huh7 cells were prepared by suspension in RIPA buffer with

protease inhibitors. The suspensions were subjected to shear stress several times using a syringe with a 25-gauge needle followed by centrifugation at 14,000 rpm for 20 min at 4 °C. For another set of experiments, nuclear and cytoplasmic proteins of cells were prepared by NE-PER extraction reagents (Thermo Fisher Scientific, Rockford, IL, USA) according to the manufacturer's protocol. The BCA protein assay kit (Thermo Fisher Scientific) was used to determine the protein concentration, and 25 μg of protein from each sample was used for SDS-PAGE. Separated proteins were transferred onto polyvinylidene difluoride (PVDF) membranes (GE Healthcare) by electroblotting, and proteins were blocked for 1 h with PBST (PBS buffer with 0.05% Tween-20) containing 4% nonfat milk powder. Immunoblots were incubated with the primary antibody followed by a horseradish peroxidase (HRP)-conjugated secondary antibody. The antibody-bound proteins were detected using an enhanced chemiluminescence (ECL) reagent (GE Healthcare), and membranes were then stripped and reprobed using an anti-α-tubulin antibody (Sigma, St. Louis, MO, USA) as a loading control.

5.2.11. Nuclear extract preparation and electrophoretic mobility shift assay (EMSA)

In order to detect DNA/protein-binding activity, nuclear proteins were prepared as described above from Huh7 cells that had been transfected with pHBV1.2 for 2 days and treated with IN-4 (**5**) (10 μg/ml) or untreated for another 2 days. For the EMSA, nuclear extracts (8 μg) were pre-incubated with or without a competitor and concomitantly mixed with 1 μg poly[dI-dC] (Sigma) and 1 μg of salmon sperm DNA (Sigma). The mixture was placed on ice for 20 min and then incubated with a ^{32}P-labeled double-stranded DNA probe for 20 min at 30 °C. The mixture was

separated on a 5% nondenatured polyacrylamide gel in 0.5 × TBE (Tris-borate-EDTA) buffer at 150 V for 90 min, and the binding shift was detected from an autoradiograph. The oligonucleotide-probe for the DNA-binding assay comprised the NF-κB consensus binding site sequence: 5′-ACTATCATCCGGAAAGCCCCCAAAAGTCCC-3′.[28]

5.2.12. Statistical analysis and quantification of data

Data are expressed as the mean and standard deviation of the mean (SD) for three independent experiments. GraphPad Prism (GraphPad Software, San Diego, CA, USA) was used for the graphical representation of results. Variance analysis and Student *t*-tests were used for data analysis. Significant differences were accepted when $p < 0.05$. Quantitative data from Northern and Western blot analyses were obtained using the computing densitometer and Total Lab Quant software (Nonlinear Dynamics, England).

Acknowledgements

This work was funded by grants from the Committee on Chinese Medicine and Pharmacy, Department of Health, Executive Yuan, Taiwan (CCMP102-RD-116) and China Medical University Hospital (DMR-103-042 and DMR-104-039). We also thank the National Science Council of Taiwan for supporting this work. The authors express heartfelt thanks to Dr. Cheng-Chan Lu for the pHBV1.2 and pHBV2 plasmids, to Dr. Hsiao-Sheng Liu for the pGAPDH plasmid, and to Dr. Cheng-Wen Lin for pAP1-Luc, pAP2-Luc, pNF-κB-Luc, and pISRE-Luc promoter-reporter constructs.

References and notes

1. Chen, D. S. *J. Hepatol.* **2009**, *50*, 805.
2. Park, N. H.; Song, I. H.; Chung. Y. H. *Postgrad. Med. J.* **2006**, *82*, 507.
3. Dény, P.; Zoulim, F. *Pathol. Biol.* **2010**, *58*, 245.
4. Ying, C.; Li, Y; Leung, C. H.; Robek, M. D.; Cheng, Y. C. *Proc. Natl. Acad. Sci. USA* **2007**, *104*, 8526.
5. Huang, T. J.; Chou, B. H.; Lin, C. W.; Weng, J. H.; Chou, C. H.; Yang, L. M.; Lin, S. J. *Phytochemistry* **2014**, *99*, 107.
6. Avent, A. G.; Hanson, J. R.; de Oliveira, B. H. *Phytochemistry* **1990**, *29*, 2712.
7. Geuns, J. M. C. *Phytochemistry* **2003**, *64*, 913.
8. Moons, N.; Borggraeve, W. D.; Dehaen, W. *Curr. Org. Chem.* **2011**, *15*, 2731.
9. Lohoelter, C.; Weckbecker, M.; Waldvogel, S. R. *Euro. J. Org. Chem.* **2013**, 5539.
10. Takasaki, M.; Konoshima, T.; Kozuka, M.; Tokuda, H.; Takayasu, J.; Nishino, H.; Miyakoshi, M.; Mizutani, K.; Lee, K. H. *Bioorg. Med. Chem.* **2009**, *17*, 600.
11. Ghose, A. K.; Viswanadhan, V. N.; Wendoloski, J. J. *J. Comb. Chem.* **1999**, *1*, 55.
12. Zhang, L.; Wang, X. J.; Wang, J.; Grinberg, N.; Krishnamurthy, D.; Senanayake, C. H. *Tetrahedron Lett.* **2009**, *50*, 2964.
13. Blum, H. E.; Galun, E.; Liang, T. J.; von Weizsacker, F.; Wands, J. R. *J. Virol.* **1991**, *65*, 1836.
14. Schuppan, D.; Jia, J. D.; Brinkhaus, B.; Hahn, E. G. *Hepatology* **1999**, *30*, 1099.
15. Huang, T. J.; Liu, S. H.; Kuo, Y. C.; Chen, C. W.; Chou, S. C. *Antivir. Res.* **2014**, *101*, 97.

16. Doria, M.; Klein, N.; Lucito, R.; Schneider, R. J. *EMBO J.* **1995**, *14*, 4747.

17. Hildt, E.; Saher, G.; Bruss, V.; Hofschneider, P. H. *Virology* **1996**, *225*, 235.

18. Kwon, J. A.; Rho, H. M. *Cell Biol.* **2002**, *80*, 445.

19. Meyer, M.; Caselmann, W. H.; Schluter, V.; Schreck, R.; Hofschneider, P. H.; Baeuerle, P. A.; *EMBO J.* **1992**, *11*, 2991.

20. Keasler, V. V.; Hodgson, A. J.; Madden, C. R.; Slagle, B. L. *J. Virol.* **2007**, *81*, 2656.

21. Cheng, S. Y.; Wang, C. M.; Hsu, Y. M.; Huang, T. J.; Chou, S. C.; Lin, E. H.; Chou, C. H. *J. Nat. Prod.* **2011**, *74*, 1744.

22. Militsina, O. I.; Strobykina, I. Y.; Kovylyaeva, G. I.; Bakaleinik, G. A.; Kataev, V. E.; Gubaidullin, A. T.; Musin, R. Z.; Tolstikov, A. G. *Russ. J. Gen. Chem.* **2007**, *77*, 285.

23. Sells, M. A.; Chen, M. L.; Acs, G. *Proc. Natl. Acad. Sci. USA* **1987**, *84*, 1005.

24. Sambrook, J.; Fritsch, E. F.; Maniatis, T., Molecular Cloning: A Laboratory Manual, second ed. Cold Spring Harbor Laboratory Press, New York, 1989.

25. Will, H.; Cattaneo, R.; Darai, G.; Deinhardt, F.; Schellekens, H.; Schaller, H. *Proc. Natl. Acad. Sci. USA* **1985**, *82*, 891.

26. Pugh, J. C.; Yaginuma, K.; Koike, K.; Summers, J. *J. Virol.* **1988**, *62*, 3513.

27. Feng, Y.; He, F.; Zhang, P.; Wu, Q.; Huang, N.; Tang, H.; Kong, X.; Li, Y.; Lu, J.; Chen, Q.; Wang, B. *Antivir. Res.* **2009**, *81*, 277.

28. Lagirand-Cantaloube, J.; Laud, K.; Lilienbaum, A.; Tirode, F.; Delattre, O.; Auclair, C.; Kryszke, M. H. *Biochem. Biophy. Res. Commun.* **2010**, *399*, 705.

Figure Legends

Figure 1. Cytotoxicity of IN-4 (**5**) against HepG2 2.2.15 and Huh7 cells. To determine the cytotoxicity, cells were plated in 96-well plates for 24 h and treated with serial dilutions (2.5–160 μg/ml) of IN-4 (**5**) for 3 days. After treatment, cells were subjected to a cytotoxic assay. Data are expressed as the mean and SD. ($n = 4$) (*$p < 0.05$ vs. untreated cells)

Figure 2. Effects of IN-4 (**5**) on (A) the secretion of hepatitis B virus (HBV) antigens and (B) replicated viral DNA levels in HepG2 2.2.15 cells. Cells were treated with various concentrations (1, 5, and 10 μg/ml) of IN-4 (**5**) for 3 days, and conditioned media were collected for the EIA analysis of HBV surface antigen (HBsAg) and HBV e antigen (HBeAg). HBV DNA was isolated from virion particles and subjected to a real-time PCR analysis. Data are expressed as the mean and SD. ($n = 3$) (*$p < 0.05$ vs. untreated cells)

Figure 3. Effects of IN-4 (**5**) on hepatitis B virus (HBV) gene expression and viral DNA replication in Huh7 cells. Huh7 cells were transfected with the pHBV1.2 plasmid for 2 days and treated with three concentrations (1, 5, and 10 μg/ml) of IN-4 (**5**) for a further 2 days. Treated cells were harvested and subjected to total RNA, protein, and DNA isolation. (A) Total RNA from transfected and treated Huh7 cells was subjected to a Northern blot analysis using HBV whole-genome DNA as a probe. GAPDH was used as an RNA loading control, and β-gal was used to detect the efficiency of each transfection. (B) Total cellular proteins were extracted, and immunoblotting was used to

detect HBV large surface antigen (LHBsAg), HBV major surface antigen (SHBsAg), HBV core antigen (HBcAg), and α-tubulin for comparison. (C) Intracellular HBV DNA was isolated and subjected to a Southern blot analysis. RC, relaxed circular; SS, single stranded; RI, replicated intermediates; HBV standard, 2 ng of 3.2-kb linear HBV genome marker. The intensity of each protein band was quantitated with a densitometer, and the relative amount was normalized to an internal control. Data shown in (A), (B), and (C) are representative of three sets of experiments.

Figure 4. Effects of IN-4 (**5**) on hepatitis B virus (HBV) gene promoter- and cellular signaling pathway-responsive promoter activity. Huh7 cells were seeded in 24-well plates for 24 h and transfected with either (A) pCore-Luc, pS-Luc, pPreS-Luc, or pX-Luc viral gene promoter reporter constructs and (B) pAP1-Luc, pAP2-Luc, pNF-κB-Luc, or pISRE-Luc promoter-responsive cellular signaling pathway elements, together with pRL-SV40. Following cotransfection for 24 h, cells were treated with IN-4 (**5**) (10 μg/ml) for another 24 h. Cellular lysates were subsequently used in a luciferase assay. Data are expressed as the mean and SD. (n = 3) (*p < 0.05 vs. untreated cells)

Figure 5. Effects of IN-4 (**5**) on NF-κB p65/p50, phospho-p65, cytoplasmic IκBα protein expressions, and DNA-binding activity of NF-κB within hepatitis B virus (HBV)-expressing Huh7 cells. (A) Huh7 cells were transfected with pHBV1.2 for 2 days and treated with three concentrations (1, 5, and 10 μg/ml) of IN-4 (**5**) for another 2 days. Proteins from the nuclear or cytoplasmic fraction were extracted, and immunoblotting was used to detect p65 and p50 of the

NF-κB protein subunit and IκBα for comparison. The proliferating cell nuclear antigen (PCNA) protein was detected in immunoblots as a control for nuclear protein expression. Data shown are representative of three sets of experiments. (B) For the DNA-binding activity assay, Huh7 cells were transfected with pHBV1.2 for 2 days and treated with IN-4 (**5**) (10 μg/ml) or left untreated. Cellular nuclear proteins were then extracted and subjected to an EMSA analysis.

Figure 6. Effect of the NF-κB signaling pathway on IN-4-mediated hepatitis B virus (HBV) inhibition. Huh7 cells were cotransfected with pHBV1.2 and with two doses (0.5 and 2.5 μg) of the pCMV-p65 plasmid for 2 days followed by treatment with IN-4 (**5**) (10 μg/ml) for another 2 days. Secreted viral particles from cells were isolated and subjected to a real-time PCR analysis of HBV DNA. For comparison, total protein of transfected and treated cells were extracted for NF-κB p65 protein immunoblot. ($n = 3$) ($^{*}p < 0.05$ vs. untreated cells)

Table 1
Anti-hepatitis B virus (HBV) activity of C4 amide-substituted isosteviol *in vitro*

Compound	TC_{50}[a]	HBsAg[b]		HBeAg[c]		DNA replication	
	(μg/ml)	IC_{50}[d] (μg/ml)	SI[e]	IC_{50}[d] (μg/ml)	SI[e]	IC_{50}[d] (μg/ml)	SI[e]
4	87.52	32.45	2.70	–	–	–	–
5 (IN-4)	65.72	10.36	6.34	11.16	5.89	5.76	11.41
6	48.45	35.64	1.36	–	–	–	–
7	19.74	4.17	4.73	12.78	1.54	7.44	2.65
8	21.65	20.85	1.04	–	–	–	–
9	14.87	10.54	1.41	–	–	–	–
10	10.54	–	–	–	–	–	–
11	18.95	–	–	–	–	–	–
12	21.19	5.57	3.80	7.38	2.87	11.20	1.89
13	22.45	18.78	1.20	–	–	–	–
14	10.78	8.45	1.28	–	–	–	–
5-FU[f]	6.12	–	–	–	–	–	–
Lamivudine[g]	205	49.13	4.17	–	–	41	5

[a] TC_{50}: 50% cytotoxic concentration in HepG2 2.2.15 cells.
[b] HBsAg: HBV surface antigen.
[c] HBeAg: HBV e antigen.
[d] IC_{50}: 50% inhibitory concentration.
[e] SI (selectivity index) = TC_{50}/IC_{50}.
[f] 5-FU (fluorouracil): positive control of cytotoxicity.
[g] Lamivudine (3TC) as the positive control.

Authors' names: Tsurng-Juhn Huang, Cheng-Lin Yang, Yu-Cheng Kuo, Yi-Chih, Chang, Li-Ming Yang, Bo-Hon Chou, Shwu-Jiuan Lin*

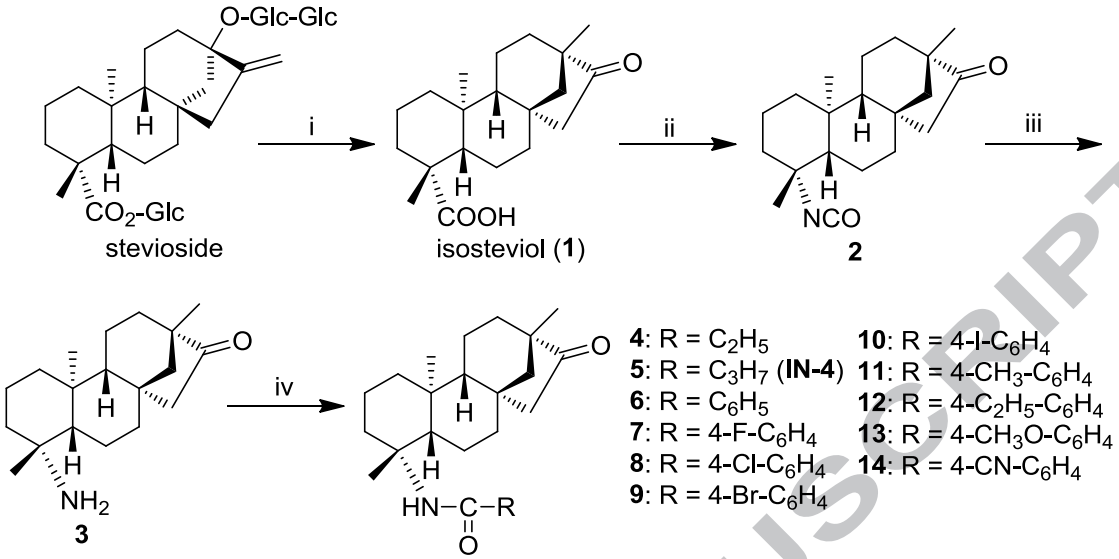

Scheme 1. Synthesis of target compounds. Reagents and conditions; i. HCl, reflux; ii. DPPA, benzene, reflux; iii. HBr, r.t.; iv. RCOCl, DMAP, Et_3N, DMF, r.t., 24 h

Scheme 1.

Authors' names: Tsurng-Juhn Huang, Cheng-Lin Yang, Yu-Cheng Kuo, Yi-Chih, Chang, Li-Ming Yang, Bo-Hon Chou, Shwu-Jiuan Lin*

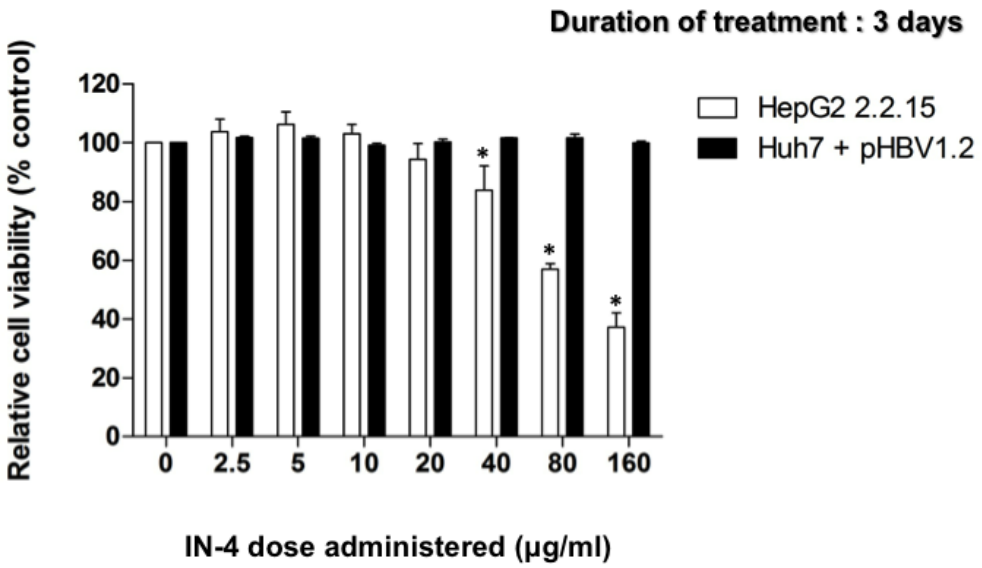

Fig. 1

Authors' names: Tsurng-Juhn Huang, Cheng-Lin Yang, Yu-Cheng Kuo, Yi-Chih, Chang, Li-Ming Yang, Bo-Hon Chou, Shwu-Jiuan Lin*

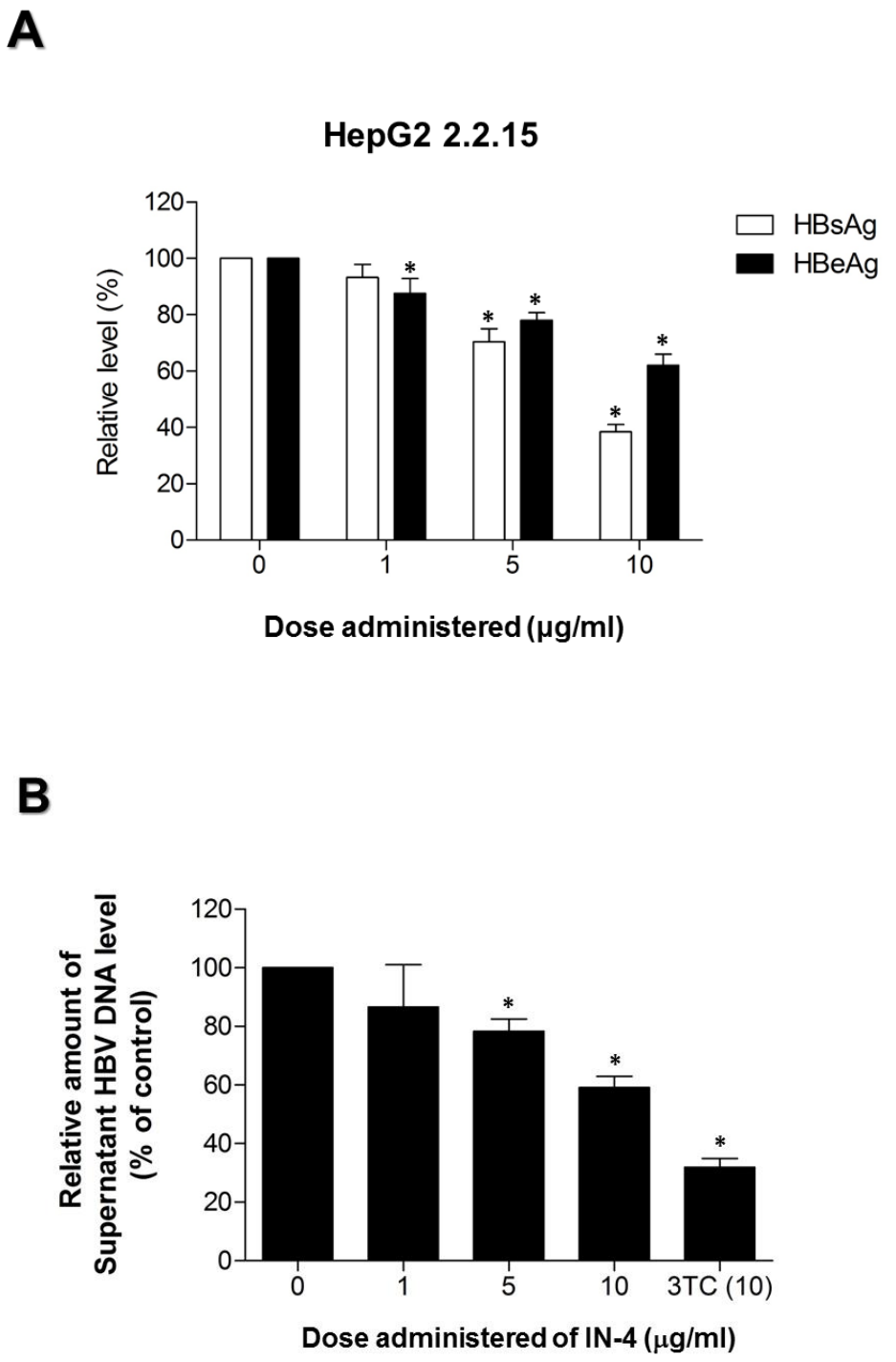

Fig. 2

Authors' names: Tsurng-Juhn Huang, Cheng-Lin Yang, Yu-Cheng Kuo, Yi-Chih, Chang, Li-Ming Yang, Bo-Hon Chou, Shwu-Jiuan Lin*

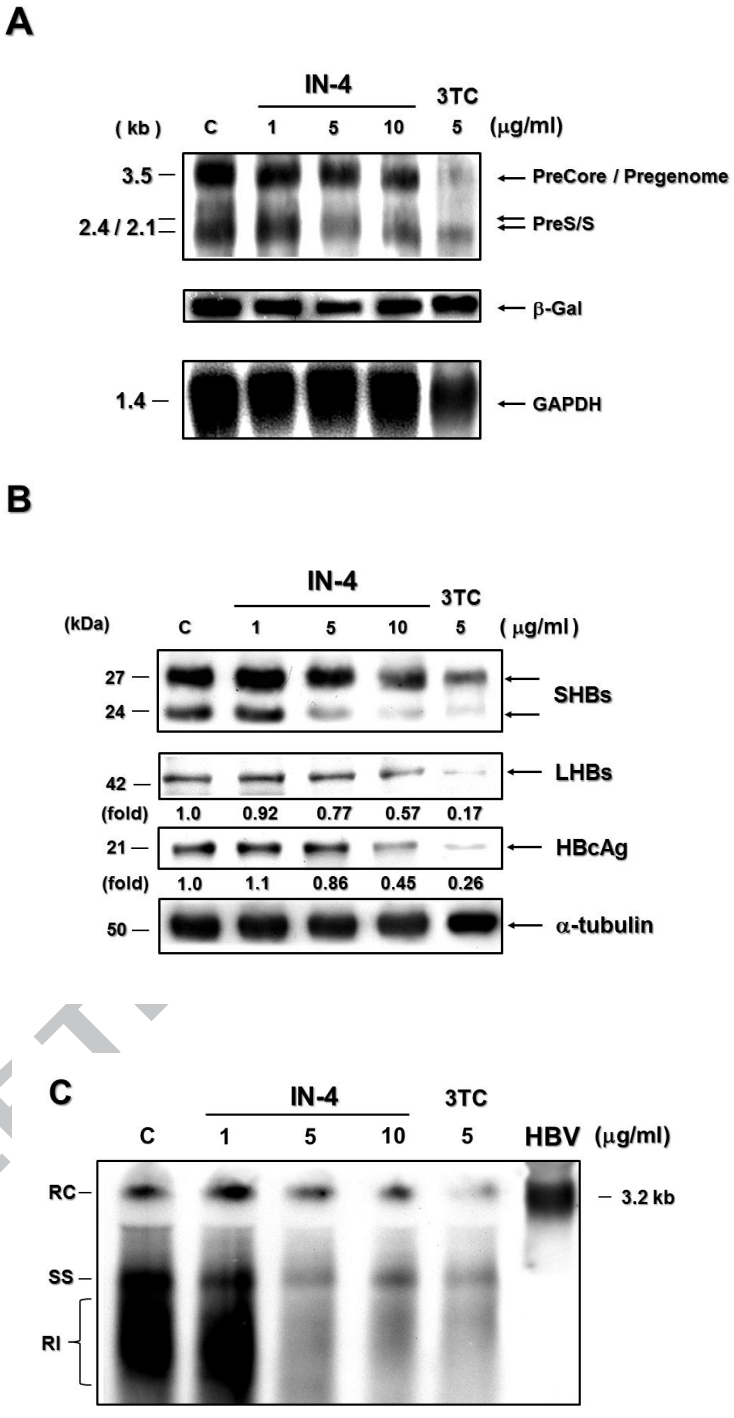

Fig. 3

Authors' names: Tsurng-Juhn Huang, Cheng-Lin Yang, Yu-Cheng Kuo, Yi-Chih, Chang, Li-Ming Yang, Bo-Hon Chou, Shwu-Jiuan Lin*

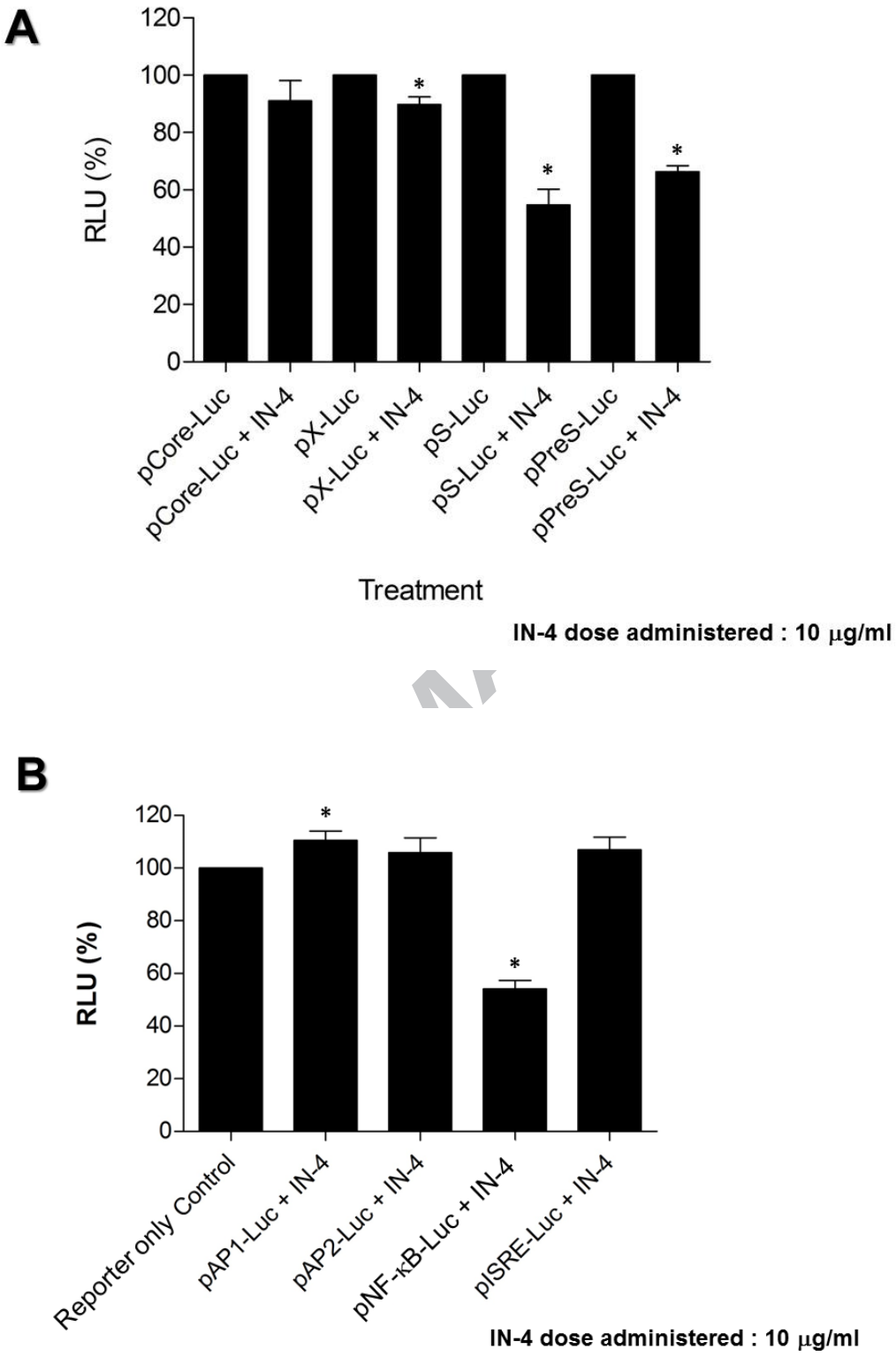

Fig. 4

Authors' names: Tsurng-Juhn Huang, Cheng-Lin Yang, Yu-Cheng Kuo, Yi-Chih, Chang, Li-Ming Yang, Bo-Hon Chou, Shwu-Jiuan Lin*

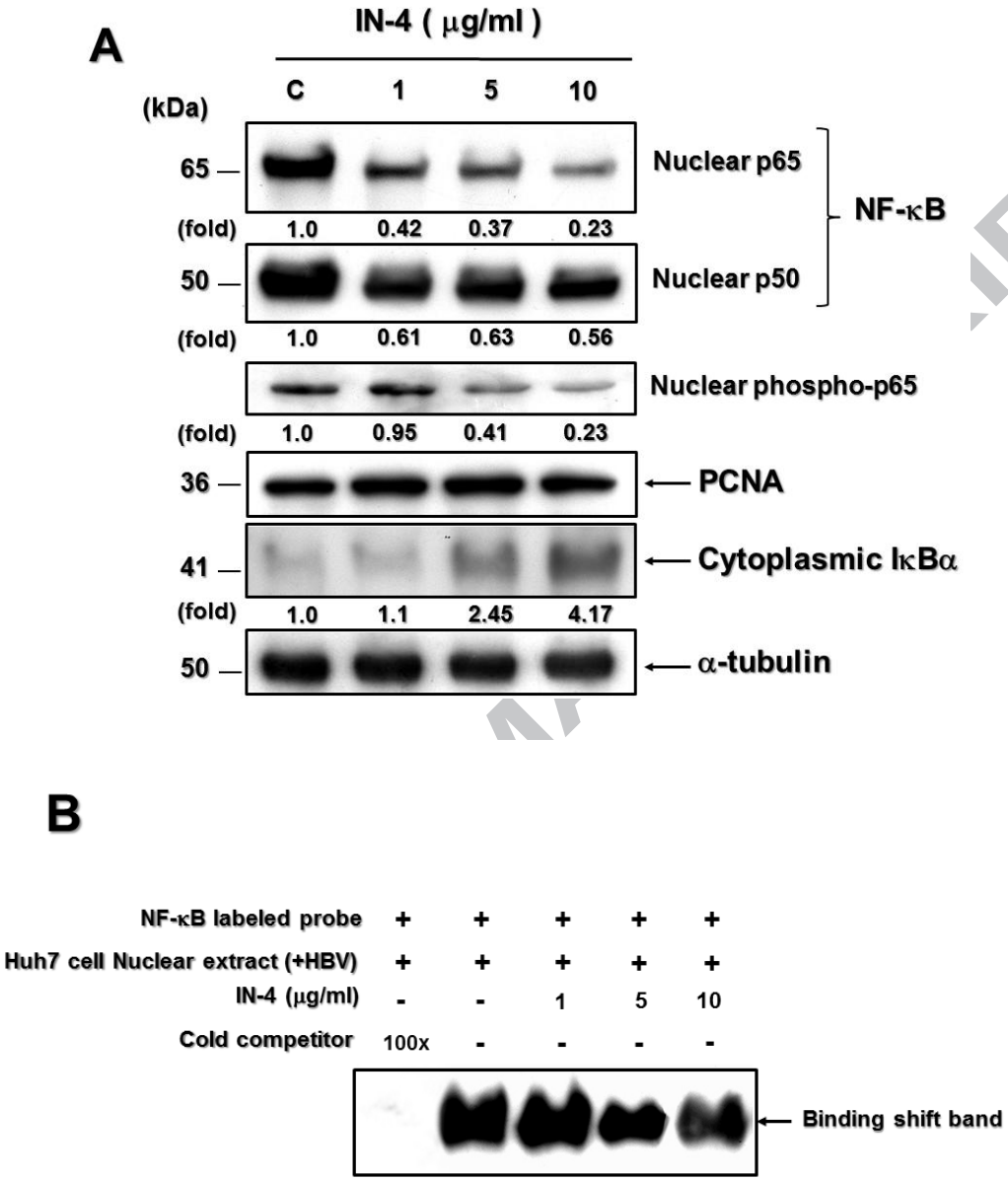

Fig. 5

Authors' names: Tsurng-Juhn Huang, Cheng-Lin Yang, Yu-Cheng Kuo, Yi-Chih, Chang, Li-Ming Yang, Bo-Hon Chou, Shwu-Jiuan Lin*

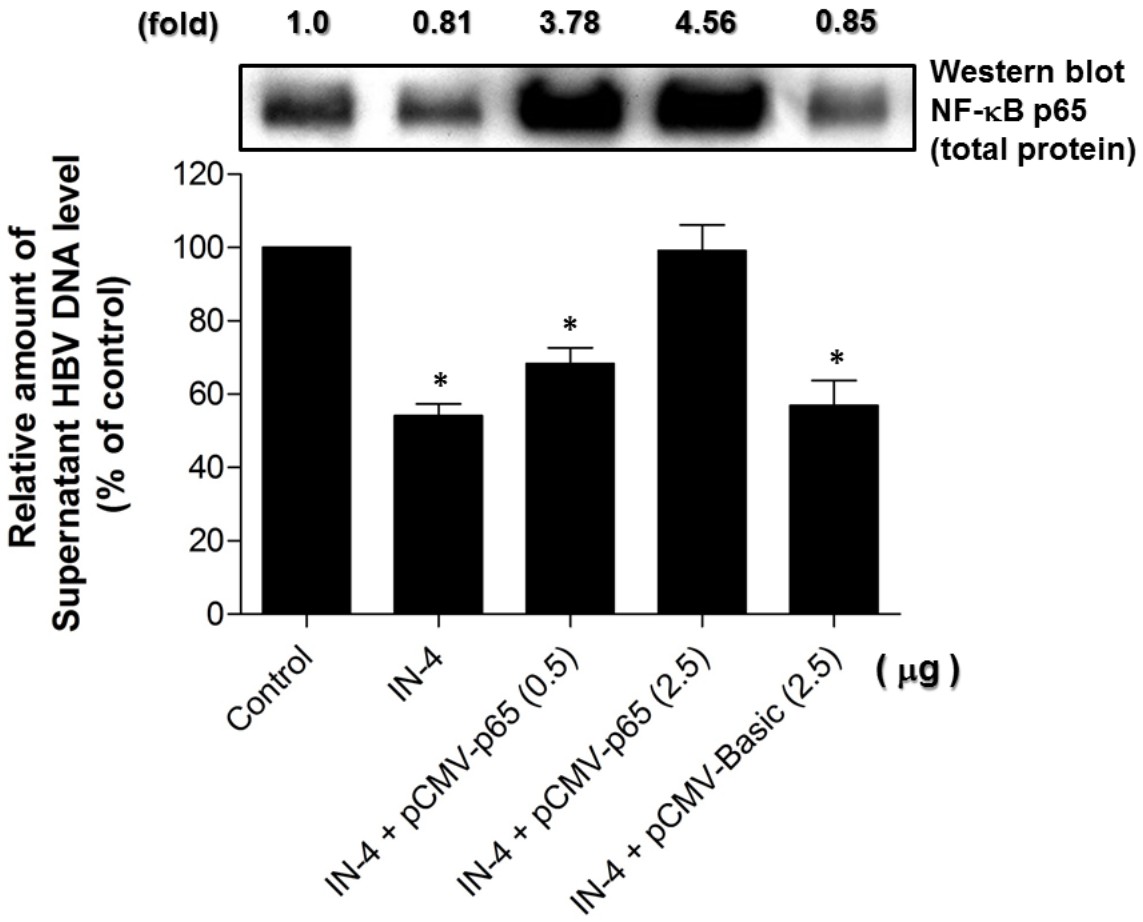

Fig. 6

Authors' names: Tsurng-Juhn Huang, Cheng-Lin Yang, Yu-Cheng Kuo, Yi-Chih, Chang, Li-Ming Yang, Bo-Hon Chou, Shwu-Jiuan Lin*

Graphic Abstract

Synthesis and anti-hepatitis B virus activity of C4 amide-substituted isosteviol derivatives

Tsurng-Juhn Huang, Cheng-Lin Yang, Yu-Cheng Kuo, Yi-Chih Chang, Li-Ming Yang, Bo-Hon Chou, Shwu-Jiuan Lin*

Among several C4 amide-substituted isosteviol derivatives, IN-4 exhibited inhibitory activity against secretion of HBsAg and HBeAg as well as inhibition of HBV DNA replication. Its action mechanism was further elucidated in HBV-transfected Huh7 cells.